2023 IEEE International Conference on Robotics and Automation (ICRA 2023)
May 29 - June 2, 2023. London, UK

A Method to Use Haptic Feedback of Laryngoscope Force Vector for Endotracheal Intubation Training

Haonan Zhou*, Siyu Yang, Lou Halamek, Thrishantha Nanayakkara, *Senior Member, IEEE,*

***Abstract*— Endotracheal intubation is a mandatory competency for most medical staff. This procedure involves opening the entrance of the patient's upper windpipe using a laryngoscope and then inserting a tube into the windpipe to supply Oxygen to the patient. This time critical intervention requires careful control of the force vector on the tongue to lift it parallel to the jaw than to push the jaw to open the mouth. However, traditional intubation training methods in which novices practice intubation on prostheses lack haptic feedback to improve force control. We designed a sensorised intubation training phantom that can provide trainees with vibrotactile feedback reflecting the laryngoscope's force on the tongue. The critical component of this phantom is a silicon rubber tongue embedded with magnets and hall effect sensors. We calibrated the hall effect sensor readings to predict the force vector exerted on the tongue with errors less than 0.5 N in the lifting and pushing directions. We conducted a controlled experiment, mainly comparing the training results between participants with and without haptic feedback. Results show a statistically significant drop in the undesired forces due to haptic feedback, and the skill is retained when tested after 24 hours without haptic feedback.**

I. INTRODUCTION

Endotracheal Intubation (EI) is a resuscitative procedure that allows healthcare professionals to insert an endotracheal tube into the trachea of a patient who is unable to breathe adequately on their own due to airway obstruction or trauma [1]. As a widely acknowledged lifesaving and life-threatening intervention, EI has become a gold standard of airway management for most physicians [2]. However, studies have shown that inexperienced healthcare professionals fail at intubation (especially in high-risk groups such as preterm neonates) more than 50% of the time; even experts are not successful 100% of the time [3]. EI involves the use of a laryngoscope that is held in the left hand and used to lift the tongue and lower jaw in order to expose the trachea. Once the trachea is visualized, an endotracheal tube is inserted into the trachea using the right hand [4]. Upon documentation of successful insertion, the unobstructed conduit keeps the airway open and connects to a ventilation bag or mechanical ventilator to provide oxygen for the patient [5]. One challenge of EI is that the duration of intubation must be as short as possible. The recommended duration of intubation by the Neonatal Resuscitation Program is limited to 20 seconds [6]. Besides, intubation requires manual dexterity and hand-eye coordination [7]; proper positioning of the fingers and hands in relation to the laryngoscope, the endotracheal tube and the patient is key to successfully securing the airway [4]. However, there is little objective, detailed, definitive data published describing the ergonomics of intubation. Similarly, intubation requires a certain amount of force and torque to be applied to the laryngoscope in order to open the entrance of the trachea. There is little published data describing the amount of force and torque to be used when intubating despite the fact that too much force and/or torque can damage the airway. All of these factors have conspired to increase difficulties to perform this procedure in patients and therefore compromised the acquisition and maintenance of this skill. Therefore, developing safe and effective training methods for this important skill is critical.

The most common intubation training method by far is the Payton approach, which involves watching educational videos about intubation, pointing out all the clinical considerations during the intubation, and finally attempting to do the intubation on a prosthesis under the supervision of senior physicians [8]. The benefit of this approach is that training the intubation on the phantom can reduce stress and cause less damage to the self-confidence of trainees when making mistakes [9].

Training to perform ET is essentially a motor learning process which involves learning an internal model of the dynamics of intubation [10]. During the process, they need to predict the force to safely lift the tongue and generate appropriate torque relying on the motor output of the new internal model. This force skill learning process can be enhanced by providing haptic feedback [11] and combining it with visual information [12] in a Bayesian integration manner [13].

Although traditional intubation training methods by standard phantoms can offer haptic and visual feedback, the actual performance of clinical intubation by healthcare professionals is still not improved sufficiently. One of the reasons is that the narrow pharynx constricts the vision of the internal airway and epiglottis anatomy [14]. Insufficient visual information could lead to oesophageal intubation and failure to recognise the anatomy, which is the most common reason for failed intubation attempts [15]. Furthermore, the haptic feedback from tactile sensors of hands is unintuitive and weak during intubation. Lack of intuitive haptic and

This work was supported in part by the Engineering and Physical Sciences Research Council (EPSRC) Grant EP/N029003/1 and Grant EP/N03208X/1.
*Corresponding author.

Haonan Zhou, Siyu Yang, and Thrishantha Nanayakkara are with the Dyson School of Design Engineering, Imperial College London, SW7 2DB London, UK (e-mail: ZHOU, haonan.zhou21@imperial.ac.uk)

Lou Halamek is with the Department of Pediatrics – Neonatology, Stanford University, USA (e-mail: halamek@stanford.edu)

visual perception extends the time it takes to skilful conduct of a successful intubation attempt and increases the possibility of injuring the patient's trachea by using an excessive intubation force or incorrect laryngoscope handling position.

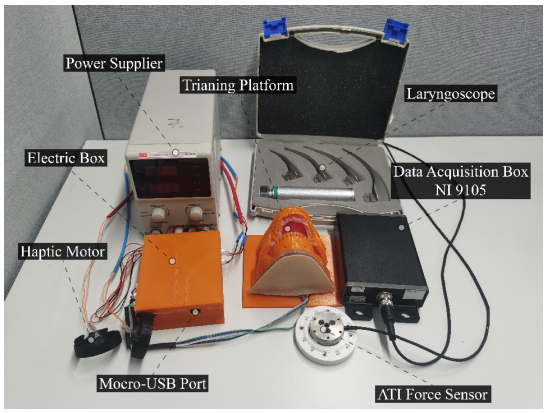

Fig. 1: The photo of all components of the endotracheal intubation training system. The ATI force sensor and data acquisition box NI 9105 are utilised only when collecting data to model the phantom.

In this paper, we introduce a new robotic intubation training phantom that can offer more robust and intuitive haptic feedback of the intubation force to the physician's arm with two vibrators. Section II will demonstrate the structure of the whole robotic intubation training system and the hardware setup used in our work. Section III describes the methods of predicting forces and transferring anticipated forces into haptic feedback. In section IV, we designed a set of controlled experiments to verify how intubation performance would be improved with this new intubation training platform. The results of the controlled experiments are described and discussed in section V and VI.

II. HARDWARE SETUP

A. Structure of The Hardware Platform

Fig. 1 demonstrates the experimental apparatus used in the system. An Arduino Nano 33 IoT acts as the controller of the entire system to process signals. An ATI Force/Torque sensor Mini 40 (F/T sensor) is used to measure the force applied to the tongue in three dimensions. The F/T sensor is connected to the computer via a National Instrument NI9205 to send the force measurement. Five SS495A Hall Linear Ratio (HLR) sensors are connected to the Arduino through AD converters to send the voltage measurement. A computer is used to read and store measurements from the F/T sensor and HLR sensors and the data collected is synchronized by Python. The computer is equipped with an Intel Core I5-2400 3.10GHz system with an internal memory of 4GB and running Windows 7(64-bit). Two vibration motors are used as actuators to provide haptic feedback to participants.

The robotic phantom used for intubation training is composed of three components: upper jaw, tongue, and lower jaw. All skeletal components of the jaws were 3D printed with PETG material (orange material shown in Fig. 1). Inside the mouth, the tissues attached to the jaws are made from Eco-Flex 30 soft silicone rubber and are bonded tightly to the 3D-printed jaws using super glue. The underside of the lower jaw is covered with a layer of soft material closely attached to both the skeleton and tissue of the lower jaw to mimic the properties of actual human skin. The tongue is made from another silicone rubber material (ECO-FLEX GEL), softer than the tissue around it. The bottom of the tongue is connected to the skin. According to the maximum degree to which the mouth can be opened, the angle between the upper jaw and lower jaw is set at 30 degrees [16].

B. Soft Tongue Haptic Sensor

In order to acquire haptic feedback data information, we designed a soft tongue tactile sensor. The sensor consists of soft tissue, permanent magnets and Hall-Effect sensors. The design schematic in cross-section is shown in Fig. 2. An orthogonal permanent magnet set with a diameter of 3mm is implanted inside the tongue, which generates a consistent magnetic field. This device uses HLR sensors divided into two groups to collect magnetic field strength data at corresponding locations in space. The group along the z-axis consists of three sensors, and the other group along the x-axis consists of two sensors. The easily deformable materials of tissue and tongue allow one to obtain haptic feedback by feeling the deformation of the soft areas of the jaw when applying force to the tongue using the laryngoscope.

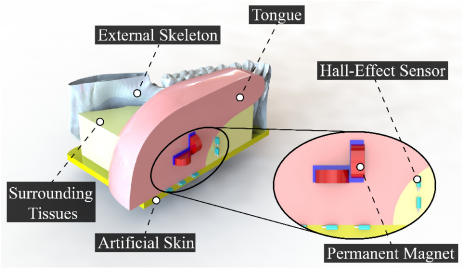

Fig. 2: The internal structure of the training phantom when no force is applied to the tongue.

III. MODELS AND METHODS

A. Force-Sensor Model

As illustrated in section II-B, all materials of the tongue, surrounding tissues and artificial skin are soft. Features of soft structure make it difficult to describe and calculate the displacement and morph, which determine the pose of the magnet set and hall-effect sensors.

On the x-z plane, poses and transformations of bodies could be represented as (x, z, θ) in a selected coordinate, where x and z are position points corresponding to the x-axis and z-axis respectively, and θ is the angle relative to the x-axis. In the meantime, (x, z, θ) can also be denoted as (l, φ, θ) which is demonstrated in (1). Because rotation joints can change angles, θ and φ, and linear joints can change lengths, l, the soft system can be modelled as a rigid body system shown in Fig. 3.

$$
\begin{aligned}
(x, z, \theta) &= (l\cos\varphi, l\sin\varphi, \theta) \\
l &= \sqrt{x^2 + z^2} \\
\varphi &= \arctan z/x
\end{aligned} \tag{1}
$$

Any force employed on the tongue would lead to morphs of the soft tongue and surrounding tissues, which would change the relative pose between sensors and magnets. To illustrate the pose relationship, transformation matrices and coordinates are utilised, where $\mathbf{C}_n$ denotes the coordinate n, matrix $\mathbf{T}$ shown in (2) denotes transformations and ${}^{M}\mathbf{T}_n$ represents the transformation matrix from coordinate $\mathbf{C}_n$ to coordinate $\mathbf{C}_M$.

$$
\mathbf{T} = \begin{bmatrix} \cos\theta & \sin\theta & x \\ -\sin\theta & \cos\theta & z \\ 0 & 0 & 1 \end{bmatrix} \tag{2}
$$

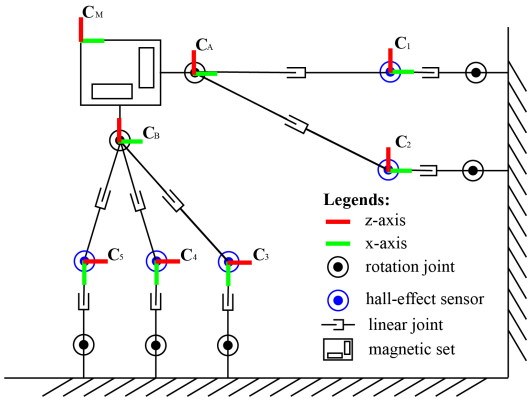

Fig. 3: The rigid-body model of the soft system.

The magnetic field generated by the orthogonal magnet set is a function of the position relative to $\mathbf{C}_M$. This function is denoted as $\mathbf{H}(x, y)$, whose output is a magnetic vector. Since the SS591A sensor can only sense scalar quantities, the values of sensors would be projections of the corresponding magnetic vector in the direction of the x-axis of the sensor coordinate. This means that sensor values are determined by position and orientation.

$$
\begin{aligned}
\mathcal{H} &\equiv (h_i), i = 1, ..., 5 \\
\mathbf{T}_m &\equiv ({}^{M}\mathbf{T}_i), i = 1, ..., 5 \\
(h_i) &= \mathbf{H}(x_i, y_i) \cdot \vec{\mathbf{x}}_i \equiv f(\mathbf{T}_m)
\end{aligned} \tag{3}
$$

As shown in (3), where (x_i, y_i) is the position of the sensor relative to the magnet coordinate $\mathbf{C_M}$, $\mathbf{T}_m$ is a tuple including every transformation matrix from corresponding sensor coordinate to magnet coordinate $\mathbf{C_M}$, and $\mathcal{H}$ is the set of the HRL sensors values, which could be defined as a function of the matrix ${}^{M}T_n$. The function between pose transformation and HRL sensors' value is denoted as $f(\cdot)$ in this paper when the pose transformation results from morph.

$$
\begin{aligned}
\mathbf{T}_h &\equiv ({}^{world}\mathbf{T}_i), i = 1, ..., 5 \\
\mathbf{F} &= \mathbf{K}({}^{world}\mathbf{T}_M, \mathbf{T}_h) \\
{}^{world}\mathbf{T}_M, \mathbf{T}_h &= \mathbf{K}^{-1}(\mathbf{F})
\end{aligned} \tag{4}
$$

The soft tongue and surrounding tissues are morphed when force is applied, which is a function of stiffness illustrated in (4), where $\mathbf{T}_h$ is a tuple including every transformation matrix from the corresponding HRL sensor coordinate $\mathbf{C}_i$ to the world coordinate $\mathbf{C}_{world}$, $\mathbf{F}$ denotes the force applied to the tongue including magnitude, direction and affected area.

$$
\begin{aligned}
{}^{M}\mathbf{T}_i &= {}^{M}\mathbf{T}_{world} \cdot {}^{world}\mathbf{T}_i \\
&= {}^{world}\mathbf{T}_M{}^{-1} \cdot {}^{world}\mathbf{T}_i, i = 1, ..., 5 \\
\mathbf{T}_m &= {}^{world}\mathbf{T}_M{}^{-1} \cdot \mathbf{T}_h
\end{aligned} \tag{5}
$$

$$
\begin{aligned}
\mathcal{H} &= f(\mathbf{T}_m) = f({}^{world}\mathbf{T}_M{}^{-1} \cdot \mathbf{T}_h) \\
&= f\left(\mathbf{K}^{-1}(\mathbf{F})\right) \\
\mathbf{F} &= \mathbf{K}\left(f^{-1}\left(\mathcal{H}\right)\right) \equiv g(\mathcal{H})
\end{aligned} \tag{6}
$$

Deriving from (3) and (4) and the transforming relationship illustrated in (5), the relationship between $\mathcal{H}$ and $\mathbf{F}$ can be denoted as a certain but unknown function $g(\cdot)$, which is defined in (6).

Considering the nonlinear distributed magnetic field, complex structure and difference in stiffness, the function is complicated to be derived analytically. In this project, this function is fitted through four different methods, which are introduced in section III-D.

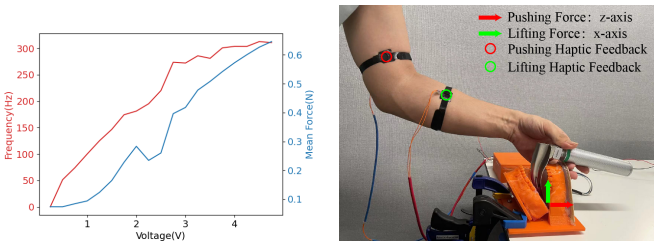

(a) F/F vs. Voltage (b) Directions and Points

Fig. 4: The haptic-related definitions. Fig. 4a shows the relationship between microactuator frequency/force (F/F) and voltage. Fig. 4b shows the directions of pushing and lifting force and corresponding haptic feedback points.

B. Haptic Feedback

Haptic feedback is an essential source of information for humans when learning and controlling movements. Physicians try to get tactile feedback in traditional airway intubation tasks by feeling the patient's jaw with the ring finger and pinky finger. However, the haptic feedback provided this way is very vague and unintuitive. Especially novice physicians do not have any idea of the relationship between what the fingers feel and the forces experienced by the patient. Providing more intuitive tactile feedback will help physicians build relevant knowledge content.

In this project, two haptic motors are utilised to provide haptic feedback to physicians. These two motors are fixed on the physician's upper arm and forearm shown as Fig. 4b. The motor's input voltage range is $0-5$ V, while the force varies from 0 to 10 N during operation. The change in the haptic

motor's vibration frequency and the average strength against the input voltage is shown in Fig. 4a. The force components in the x-axis and z-axis directions are mapped to the input voltages of the two motors by the function shown in (7). Positions of haptic feedback points and force direction are shown in Fig. 4b.

$$v = \frac{5}{1 + e^{-(F-6)}} = \frac{5e^{(F-6)}}{e^{(F-6)} + 1} \tag{7}$$

C. Data Collection

To fit models regressing the function $\mathbf{F} \equiv \mathbf{g}(\mathcal{H})$, values from hall-effect sensors and corresponding force label on each axis are needed.

Before collecting data, we must set up hardware, build communication channels and calculate static bias. The mouth phantom, the primary hardware component, is mounted on the ATI F/T sensor which is fixed on the table and connected to the computer through data acquisition box NI 9105 with a 1000Hz sampling rate. Outputs of hall-effect sensors are measured by a 12-bits Analog/Digital Converter (ADC), which sends the data to the Arduino through I2C communication at a 200Hz sampling rate. The Arduino utilises Serial communication sending the data to the computer. The computer calculates the static bias based on 1000 samples before collecting data.

After setting static bias, forces are exerted on the tongue through a laryngoscope. Because the phantom is fixed and there is no other force interface, according to Newton's first law, the force measured by the sensor is equal in magnitude and opposite in direction to the force applied to the tongue.

Then, raw data from the Hall-Effect sensor and F/T sensor are collected at 200Hz and pre-processed. All data from each Hall effect sensor are normalised, while the data from the force sensors are inverted on each axis before storing to the data set. The data set was divided into a training set and a test set in a 9:1 ratio after the data set was built.

D. Force Prediction

As introduced in section III-A, the function $\mathbf{F} = g(\mathcal{H})$ cannot be easily analyzed. To obtain the map from $\mathcal{H}$ to F, we considered four data-driving methods. They are Linear Regression (LR), Support Vector Regression (SVR), Neural Network (NN), and Random Forest Regression (RFR).

The LR model is derived through the least squares method.

The SVR model is optimised by the RBF kernel whose parameter γ is set to $(5\mathrm{var}(\mathrm{H}))^{-1}$, where $var(\cdot)$ denotes the function of variance and 5 is the number of the input features. The parameter epsilon is set to 0.1.

The NN model in this project is a five-layer network, including an input layer, three hidden layers and an output layer. Those three hidden layers consist of 30, 50, and 10 cells, respectively and are activated by the nonlinear Sigmoid function. This network is trained by Adam optimiser for 200 episodes, and the data batch size is 32.

The RFR model consists of 50 trees in the forest, and all the trees would be expanded until all leave nodes are pure or contain less than two samples.

All the models in this section utilise $L1$ defined in (8) as the loss function, where $\hat{y}_i$ N is the predicted force and y_i N is the actual force. In this project $i = 0, 1$, denoting the pushing force and lifting force, respectively.

$$L1 \equiv \left| \sum \hat{y}_i - y_i \right| \tag{8}$$

Table I shows time consumed by sampling and force prediction utilising different models. The time consumed by model calculations is defined as from data acquisition to output of the predicting data. The sampling duration is transferred from the sampling rate, which is 200Hz. This determines that there is a 5ms delay of the haptic feedback, which has been proved, in [17], would not hinder the feedback benefit.

Fig. 5 shows $L1$ errors on each axis for 100 samples calculated by all four models. The RFR is the most accurate model with $mean(L1|\mathbf{RFR}) = (0.13, 0.17)$ and $std(L1|\mathbf{RFR}) = (0.16, 0.22)$, where $(L1|\mathbf{RFR})$ denotes the L1 error of RFR model on each axis, $mean$ and std denote average value and standard deviation respectively. Performances for other models are $mean(L1|\mathbf{LR}) = (1.3, 2.0)$, $mean(L1|\mathbf{SVR}) = (0.78, 1.11)$, and $mean(L1|\mathbf{NN}) = (0.62, 0.74)$.

Combining the model's performance and the calculating time shown in Table I, RFR is the chosen model to implement on the platform because the consumed time is less than the sampling duration and is of the highest performance.

TABLE I: The time spent by sampling and force prediction utilising different models.

	LR	SVR	NN	RFR	Sampling Duration
Time(ms)	0.1	1.2	0.2	3.1	5.0

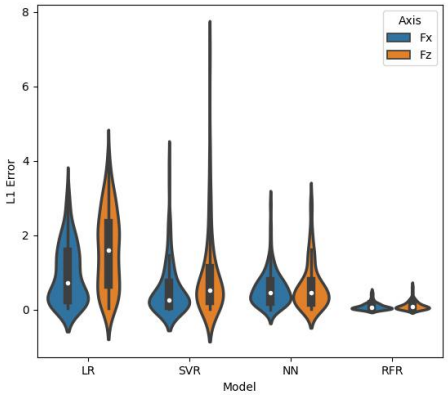

Fig. 5: The comparison of different models to predict Laryngoscope force on the tongue. The considered models are: Linear Regression (LR), Support Vector Regression (SVR), Neural Network (NN), and Random Forest Regression (RFR).

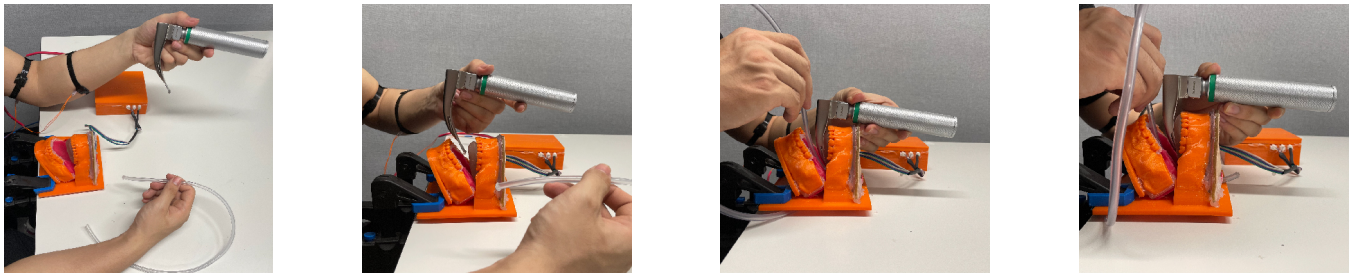

(a) Preparing (b) Starting (c) Processing (d) Completed

Fig. 6: Four steps of one experiment trial.

IV. EXPERIMENT

In this experiment, 14 participants were enrolled with informed consent and divided into the experimental and control group. The 14 participants are all 22 to 25 years old except for one 52-year-old in the experimental group. There is one mixture-hand user in each group while all others are right-hand users. The only significant difference between the two groups was whether or not haptic feedback was provided. The experimental protocol was approved by the low risk ethics committee of the Dyson School of Design Engineering, Imperial College London.

For clinical purposes, three features are chosen to evaluate one trial. They are the max lifting force, max pushing force and the time consumed to complete intubation. Those features of every trial are shown in Fig. 8, where the shaded area represents the standard error around the average. Mann-Whitney u-test [18] is a nonparametric test usually used to compare differences between two independent groups. We used it to identify the statistical difference in the features between the experimental and control groups. The test result-related data are illustrated in Table II.

A. Control Trials Design

This experiment aims to prove that the force feedback provided by the motor vibrators can improve intubation training. The design of the experiment process is illustrated in Fig. 7.

In the first part of the experiment, participants are divided into groups: the experimental group and the control group. Both groups will first be asked to watch an intubation demonstration video by Lou Halamek to learn how to operate the intubation. Afterwards, the experimental group would perform intubation twenty times on the training phantom with the haptic feedback provided. In contrast, the participants in the control group will do that without any haptic feedback. The laryngoscope force vector and the time consumed during each intubation was recorded. The data recorded are utilised in short-term learning analysis. These 20 trials are named as the short experiment set (SES).

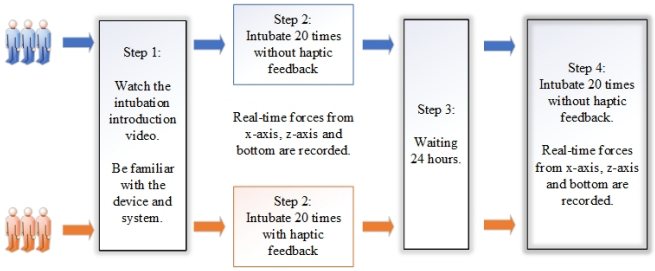

Fig. 7: The process design of control trials. The group in blue denotes the control group, while the amber group denotes the experimental group. Boxes in black shadow mean the step for both groups.

After 24 hours, every participant in both groups is recalled to do another set of trials without haptic feedback. The laryngoscope force vector and the time consumed during each intubation are entirely re-recorded. These data is utilised in long-term learning analyse. The 20 trials after 24 hours are denoted the long experiment set (LES).

B. Steps for A Single Trial

Four landmark steps are defined in this experiment for a single trial: preparing, starting, processing and completed. Photos in Fig. 6 show the state of each of these four steps.

In the preparing state, the participant should take the tools out of the training phantom and wait for the command to start the trail. The participant receives the instruction to start

TABLE II: The Mann-Whitney U-test results. T1 and T2 denote the first eight trials and last eight trials of the SES, and T3 and T4 denote those of the LES, respectively.

		Mean				Standard Deviation				p-Value			
		T1	T2	T3	T4	T1	T2	T3	T4	T1	T2	T3	T4
Lifting Force	Experimental Group	8.64	8.48	8.04	8.23	1.93	2.31	2.14	1.71	1.33e-03	3.03e-03	8.48e-08	1.12e-08
	Control Group	9.97	9.76	10.21	10.33	2.02	2.05	1.67	1.62				
Pushing Force	Experimental Group	8.34	6.97	6.38	6.49	2.27	2.28	1.85	1.64	0.10*	1.18e-03	1.61e-04	1.16e-04
	Control Group	8.55	8.53	7.62	7.74	1.53	1.81	1.35	1.26				
Time	Experimental Group	12.13	8.56	5.77	5.51	8.00	3.38	2.45	2.45	8.61e-04	3.60e-03	0.01	0.45*
	Control Group	19.94	12.85	7.82	5.31	14.50	8.71	4.58	2.27				

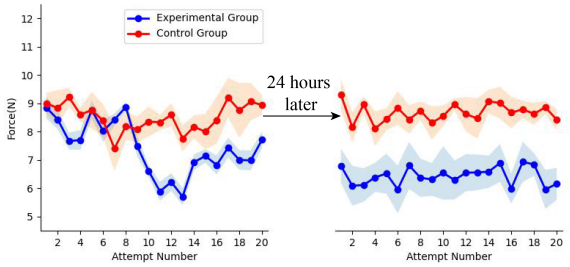

(a) Pushing Force

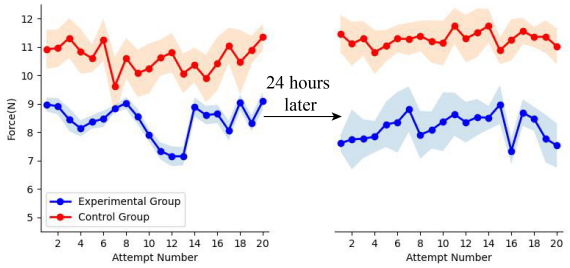

(b) Lifting Force

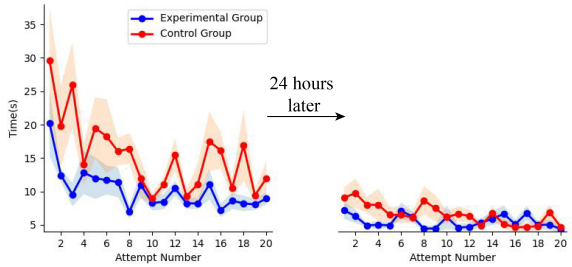

(c) Intubation Time

Fig. 8: How do the pushing force, lifting force and time consumed by intubating data change along trials.

and immediately begins the intubation operation. Timing will start when the laryngoscope enters the mouth of the phantom, as shown in Fig. 6b. When it is processed as Fig. 6c, the laryngoscope force vector would be recorded at 50 Hz until the intubation is completed.

V. RESULTS

In Fig. 8a, the pushing forces of two groups are close and mixed in the first eight trails (T1) of SES. After the eighth trial, the experimental group data starts to reduce while the control group remains. Regarding LES, both pushing and lifting forces of the experimental group were smaller than those of the control group. Comparing SES and LES, the control group had similar pushing in all trials in both SES and LSE. However, the experimental group had significantly lower data in LSE than in SES.

The lifting forces shown in Fig. 8b for both groups remain stable. The values of the experimental group are always smaller than those of the control group, and this difference tended to be constant.

The times consumed shown in Fig. 8c are typical learning curves which are large at first and reduce gradually. The initial values are smaller for the experimental group. With trials repeated, the times consumed by the two groups gradually become closer. And this can also be derived from p-values shown in Table II, where p-values of $T4 > T3 > T2 > T1$.

VI. DISCUSSION

Although excessive force and/or torque can damage the airway, there is little published data describing the amount of force and torque to be used during intubation. Historically, intubation has been described and assessed by highly subjective ("feel") and relatively crude objective ("in" or "out") criteria. This reliance on subjective rather than sophisticated objective performance markers severely impairs both the initial acquisition and the maintenance of this critically important skill.

Authors in [19] review the video recordings of intubation attempts by three groups of people: residents, follow and consultants. The results show that the success rate and mean duration of intubation for consultants are 86% and 25 seconds, which are much better than follows (78% success rate and 32 seconds) and residents (24% success rate and 49 seconds).

Our results show that the experimental group always had less lifting force than the control group. The forces of the experimental group rarely exceed 9 N, while the forces of the control group are around 11 N. Mean values of the lifting force remain stable across trials. The p-values for lifting force remained < 0.01 while it was still reducing.

The pushing forces of the two groups are close $p > 0.01$ in the T1 period. However, after eight trials, the experimental group started to reduce the pushing force while the control group remained. After 24 hours, when the control group maintained the former performance, the experimental group had learned an excellent ability to reduce their pushing force. The p-value of pushing force in T1 shown in Table II was 85 times greater than that in T2 and 617 and 862 times greater than at stages T3 and T4 respectively.

The consumed time curve is a typical learning curve where the experimental group learn faster than the control group. However, their final stable value tends to be the same. The Mann-Whitney u-test result shows that at the T4 period, the consumed times of the experimental and control groups are almost equally distributed, which can be approved by the p-value 0.45.

VII. CONCLUSIONS

This paper proposes a sensorised mouth phantom to provide haptic feedback for endotracheal intubation training. Experiment results using human participants show that the haptic feedback of lifting and pushing force by the laryngoscope on the tongue leads to a staistically significant reduction in pushing force against the jaw compared to a control group who did not receive haptic feedback of the laryngoscope force vector. This skill is retained after 24 hours when tested without haptic feedback. Moreover, there is a reduction of time taken to complete the intubation procedure after a 24 hour break. This could come from motor memory consolidation during the break.

REFERENCES

[1] T. Ezri and R. D. Warters, "Chapter 15 - indications for tracheal intubation," in *Benumof's Airway Management (Second Edition)*, second edition ed., C. A. Hagberg, Ed. Philadelphia: Mosby, 2007, pp. 371–378. [Online]. Available: https://www.sciencedirect.com/science/article/pii/B9780323022330500226

[2] R. Coimbra, D. P. Davis, and D. Hoyt, "Chapter 10 - prehospital airway management: Intubation, devices, and controversies," in *Current Therapy of Trauma and Surgical Critical Care*, J. A. ASENSIO and D. D. TRUNKEY, Eds. Philadelphia: Mosby, 2008, pp. 58–63. [Online]. Available: https://www.sciencedirect.com/science/article/pii/B978032304418950014X

[3] S. Chawla, G. Natarajan, S. Shankaran, B. Carper, L. P. Brion, M. Keszler, W. A. Carlo, N. Ambalavanan, M. G. Gantz, A. Das *et al.*, "Markers of successful extubation in extremely preterm infants, and morbidity after failed extubation," *The Journal of pediatrics*, vol. 189, pp. 113–119, 2017.

[4] A. C. Alvarado and P. Panakos, "Endotracheal tube intubation techniques," in *StatPearls*. Treasure Island (FL): StatPearls Publishing, Jan. 2022.

[5] S. B. Stone, "Chapter 12 - endotracheal intubation," in *Essential Clinical Procedures (Second Edition)*, second edition ed., R. W. Dehn and D. P. Asprey, Eds. Philadelphia: W.B. Saunders, 2007, pp. 145–164. [Online]. Available: https://www.sciencedirect.com/science/article/pii/B9781416030010500162

[6] J. Kattwinkel and D. Boyle, *Textbook of neonatal resuscitation*. Amer Academy of Pediatrics, 2006, vol. 355.

[7] C. W. Buffington, S. D. MacMurdo, and C. M. Ryan, "Body position affects manual dexterity," *Anesthesia & Analgesia*, vol. 102, no. 6, pp. 1879–1883, 2006.

[8] M. Zamani, M. Nasr-Esfahani, M. Forghani, M. A. Sichani, and A. Omid, "Endotracheal intubation training to medical practitioners: Comparison of the modified 4-step payton's training method and halsted's training method in a simulated environment," *Journal of Education and Health Promotion*, vol. 9, 2020.

[9] O. A. Alsaied, J. G. Chipman, and M. E. Brunsvold, "Simulation in critical care," in *Comprehensive Healthcare Simulation: Surgery and Surgical Subspecialties*. Springer, 2019, pp. 253–261.

[10] R. Shadmehr and F. A. Mussa-Ivaldi, "Adaptive representation of dynamics during learning of a motor task," *Journal of neuroscience*, vol. 14, no. 5, pp. 3208–3224, 1994.

[11] D. Morris, H. Tan, F. Barbagli, T. Chang, and K. Salisbury, "Haptic feedback enhances force skill learning," in *Second Joint EuroHaptics Conference and Symposium on Haptic Interfaces for Virtual Environment and Teleoperator Systems (WHC'07)*. IEEE, 2007, pp. 21–26.

[12] M. O. Ernst and M. S. Banks, "Humans integrate visual and haptic information in a statistically optimal fashion," *Nature*, vol. 415, no. 6870, pp. 429–433, 2002.

[13] G. Carboni, T. Nanayakkara, A. Takagi, and E. Burdet, "Adapting the visuo-haptic perception through muscle coactivation," *Scientific reports*, vol. 11, no. 1, pp. 1–7, 2021.

[14] H. Langenstein and G. Cunitz, "Difficult intubation in adults," *Der Anaesthesist*, vol. 45, no. 4, pp. 372–383, 1996.

[15] J. E. O'Shea, P. Loganathan, M. Thio, C. O. F. Kamlin, and P. G. Davis, "Analysis of unsuccessful intubations in neonates using videolaryngoscopy recordings," *Archives of Disease in Childhood-Fetal and Neonatal Edition*, vol. 103, no. 5, pp. F408–F412, 2018.

[16] I. Calder, J. Picard, M. Chapman, C. O'Sullivan, and H. A. Crockard, "Mouth opening: a new angle," *The Journal of the American Society of Anesthesiologists*, vol. 99, no. 4, pp. 799–801, 2003.

[17] E. Ivanova, J. Eden, S. Zhu, G. Carboni, A. Yurkewich, and E. Burdet, "Short time delay does not hinder haptic communication benefits," *IEEE Transactions on Haptics*, vol. 14, pp. 322–327, 4 2021.

[18] H. B. Mann and D. R. Whitney, "On a test of whether one of two random variables is stochastically larger than the other," *The annals of mathematical statistics*, pp. 50–60, 1947.

[19] C. P. O'Donnell, C. O. F. Kamlin, P. G. Davis, and C. J. Morley, "Endotracheal intubation attempts during neonatal resuscitation: success rates, duration, and adverse effects," *Pediatrics*, vol. 117, no. 1, pp. e16–e21, 2006.